

Graphical analysis for gel morphology II. New mathematical approach for stretched exponential function with $\beta > 1$

This article has been downloaded from IOPscience. Please scroll down to see the full text article.

2005 J. Phys.: Condens. Matter 17 6319

(<http://iopscience.iop.org/0953-8984/17/41/003>)

View [the table of contents for this issue](#), or go to the [journal homepage](#) for more

Download details:

IP Address: 129.252.86.83

The article was downloaded on 28/05/2010 at 06:09

Please note that [terms and conditions apply](#).

Graphical analysis for gel morphology II. New mathematical approach for stretched exponential function with $\beta > 1$

Chihiro Hashimoto¹, Pascal Panizza², Jacques Rouch² and Hideharu Ushiki¹

¹ Graduate School of Bio-Application and System Engineering (BASE), Tokyo University of Agriculture and Technology, 3-5-8 Saiwai-cho, Fuchu-shi Tokyo 185-0054, Japan

² Centre de Physique Moléculaire Optique et Hertzienne (CPMOH), Bordeaux I University, 351 Cours de la Liberation 33405 Talence, France

Received 4 July 2005

Published 30 September 2005

Online at stacks.iop.org/JPhysCM/17/6319

Abstract

A new analytical concept is applied to the kinetics of the shrinking process of poly(*N*-isopropylacrylamide) (PNIPA) gels. When PNIPA gels are put into hot water above the critical temperature, two-step shrinking is observed and the secondary shrinking of gels is fitted well by a stretched exponential function. The exponent β characterizing the stretched exponential is always higher than one, although there are few analytical concepts for the stretched exponential function with $\beta > 1$. As a new interpretation for this function, we propose a superposition of step (Heaviside) function and a new distribution function of characteristic time is deduced.

1. Introduction

In a wide variety of applications in complex systems, including glass-forming liquids and polymers, several non-exponential functions have been proposed to describe the relaxation curve from dielectric spectroscopies, nuclear magnetic relaxation measurements, quasielastic neutron scattering and so on. Many researchers have shown the usefulness of the Kohlrausch–Williams–Watts (KWW) function [1, 2]

$$I(t) = \exp\left(-\left(\frac{t}{\tau_{\text{KWW}}}\right)^\beta\right), \quad (1)$$

where τ_{KWW} is a characteristic time and the exponent β ranges between zero and one. This function is also called a stretched exponential. The meaning of the KWW function itself has been discussed from the viewpoint of fractal structure [3], while there are many trials that a relaxation curve such as KWW function can be described by a superposition of exponential

functions as follows. Assuming a distribution of characteristic time τ as $D(\tau)$, $I(t)$ is given by

$$I(t) = \int_0^{\infty} D(\tau)F(t, \tau) d\tau, \quad (2)$$

where $F(t, \tau)$ is an elemental function. When $F(t, \tau)$ is expressed by

$$F(t, \tau) = \exp\left(-\left(\frac{t}{\tau}\right)\right), \quad (3)$$

equation (2) means the Laplace transform. Humbert [4] showed that $D(\tau)$ in equation (2) is formally expressed by

$$D(\beta, \tau) = -\frac{1}{\pi} \sum_{k=0}^{\infty} \frac{(-1)^k}{k!} \sin(\pi\beta k) \frac{\Gamma(\beta k + 1)}{\tau^{\beta k + 1}}, \quad 0 < \beta \leq 1. \quad (4)$$

Moreover, the CONTIN program is justified to be one of the most faithful algorithms to solve the Laplace transform among some attempts to deduce $D(\tau)$ itself directly from the observed relaxation curve [5, 6]. The KWW function is a time-domain function, whereas the following Havriliak–Nagami (HN) function applies for the frequency domain function [7].

$$I^*(\omega) = \frac{1}{[1 + (i\omega\tau_{\text{HN}})^{\alpha}]^{\gamma}} \quad (5)$$

α and γ are parameters ranging between zero and one, and τ_{HN} is a characteristic relaxation time. The Debye function is recovered again in case of the HN function with $\alpha = \gamma = 1$. The Cole–Cole function corresponds to the case $0 < \alpha < 1$ and $\gamma = 1$ [8], and the Cole–Davidson to the $\alpha = 1$ and $0 < \gamma < 1$ [9]. The HN and KWW functions are not exact Fourier transforms of each other, and the HN function is a more versatile function than the KWW one. Gomez and Alegria compared KWW, HN and the following Rajagopal distribution [10] functions for the fit to the dielectric relaxation data [11].

$$D(\beta, \tau) = \ln 10 \left(\frac{\beta}{2\pi(1-\beta)}\right)^{1/2} \left(\beta \frac{\tau}{\tau_0}\right)^{\beta/2(1-\beta)} \exp\left[-(1-\beta)\left(\beta \frac{\tau}{\tau_0}\right)^{\beta/(1-\beta)}\right], \quad (6)$$

$$0 < \beta \leq 1.$$

In the field of glass-forming systems, there has been a strong controversy about the real origin of such a relaxation curve [12, 13].

Some polymer gels show an enormous volume change by temperature, solvent composition, etc. Poly (*N*-isopropylacrylamide) (PNIPA) gels are well known as nonionic polymer gels which show a large volume change in water by temperature [14]. After a large temperature jump over the critical point, PNIPA gels showed a two-step shrinking, and the secondary shrinking of gels was expressed well by a stretched exponential function in the previous paper [15]. The exponent characterizing the stretched exponential β was always greater than one and even higher than two. The discussion about a stretched exponential with $\beta > 1$ is sparse compared to that with $\beta < 1$. In this report, a new mathematical approach for the stretched exponential with $\beta > 1$ is proposed by introducing a distribution function. A distribution function can be considered to be getting more and more important in order to describe the experimental data in various measurements, for example, dielectric relaxation, ultrasonic, rheology, light scattering measurements, and even fluorescence spectroscopy [16].

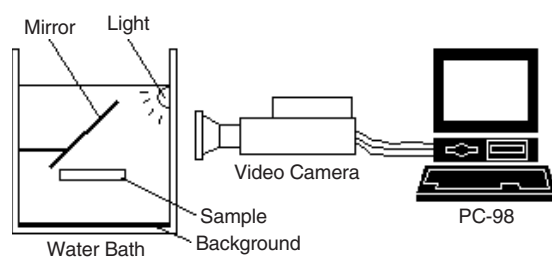


Figure 1. Experimental apparatus.

2. Experimental details

2.1. Sample

The experimental procedure was same as in the previous article [15]. An aqueous solution of *N*-isopropylacrylamide (NIPA; monomer; 655 mM), *N,N'*-methylenebisacrylamide (BIS; cross-linker), *N,N,N',N'*-tetramethylethylenediamine (TEMED; accelerator) and ammonium persulfate (APS; initiator) was polymerized between glass plates with a spacer; thickness was about 0.1, 0.2, 0.3 and 0.4 mm. It was undisturbed at 20 °C for one day, then the synthesized sheet-like gels were washed several times with a large amount of distilled water for about a week. By cutting the sheet-like gels with a cookie cutter, disc-like gels were prepared and put into a 2.0 mm thickness cell filled with distilled water and sealed with epoxy resin. The critical temperature (T_c) was close to 34.1 °C based on cloud point measurement. The cross-linkage density of the gel is given by $2N_c/(N_c + N_m)$, where N_c and N_m are molar concentrations of cross-linker and monomer, respectively, and was obtained as 8.8×10^{-3} .

2.2. Measurement

The sample cell was immersed in a thermostatted water bath and lighted from above by a white light source as shown in figure 1. The shrinking process of the gels was studied at various destination temperatures, from T_c to $T_c + \Delta T$ with $\Delta T = 0.0, 0.2, 0.4$ and 1.0 °C. It took 2–3 min to reach the desired temperature in the sample cell. Images of the gels were intermittently recorded using a digital video camera (Sony Co.: DCR VX-1000) and converted into RGB form files throughout the video board (I-O DATA: GV-98X) at a light intensity resolution of 256 and a spatial resolution of 320×200 dots. From the G (green) plane, the graphics were transferred to an MS-DOS personal computer by our original software.

Programs for graphical analysis and curve fitting were made by Turbo PASCAL (Borland). Various fitting functions can always be estimated for all data curves using the nonlinear-least-squares method based on the quasi-Marquardt algorithm as a software part of PLASMA. Calculations were carried out on a personal computer (NEC: PC-9821V13) with a co-processor for numerical calculations (Intel: 8087/80287).

3. Results and discussion

3.1. Graphical analysis

When PNIPA gels are immersed in water above the critical temperature, the transparent gels shrink and become opaque due to its intense multiple scattering. After the gels shrink, the white slowly disappears with time and finally the gels become completely transparent. This

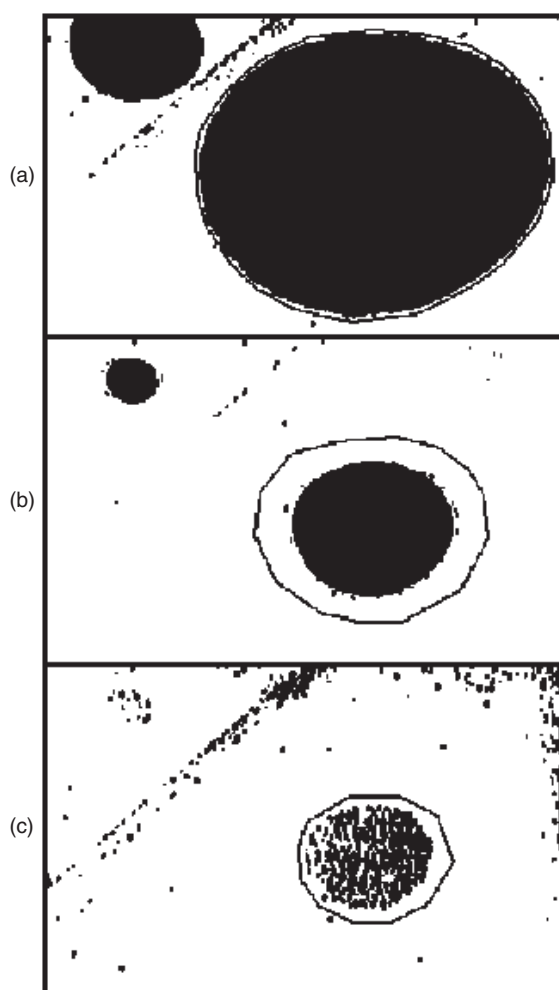


Figure 2. Temporal change in clipping images of disc-like PNIPa gels after temperature jump. The time after the jump at $\Delta T = 1.0^\circ\text{C}$ is (a) 3 min, (b) 60 min and (c) 1296 min. The thickness and diameter of gels are about 0.4 and 61 mm, respectively.

final state is regarded as the equilibrium state. Since PNIPa gels are transparent at first, we cannot get images of disc-like gels clearly using a video camera. So a white plastic disc was used to estimate the initial size of the gel. On increasing scattered light on the gels, the disc-like gels become white and can be observed clearly against a black background. A clipping procedure was used to process the image after using a digital low pass filter to reduce the effects of noise: we count zero if the intensity of a pixel is less than or equal to 63 (background) and one if comprised of 64 and 255 (gels). Using such a procedure, we obtain black and white images of the disc-like gels as shown in figure 2. The black domain due to whitening of gels becomes gradually smaller with time. In figures 2(c), the gels are spotted with black and white, indicating that gels are randomly spotted with white and transparent parts when the whitening disappears. When the gels become finally transparent, black domains disappear completely.

Here we introduce a parameter $S(t)$ to express the temporal change of the area of disc-like gels. As shown in figure 2, the number of black dots within a closed curve line defines $S(t)$, normalized to one at the initial value of area obtained using a white plastic disc of size the same as before shrinking. The plot of $S(t)$ as a function of time for various thickness gels is shown in figure 3. $S(t)$ decreases monotonically and remains constant for a while, then decreases

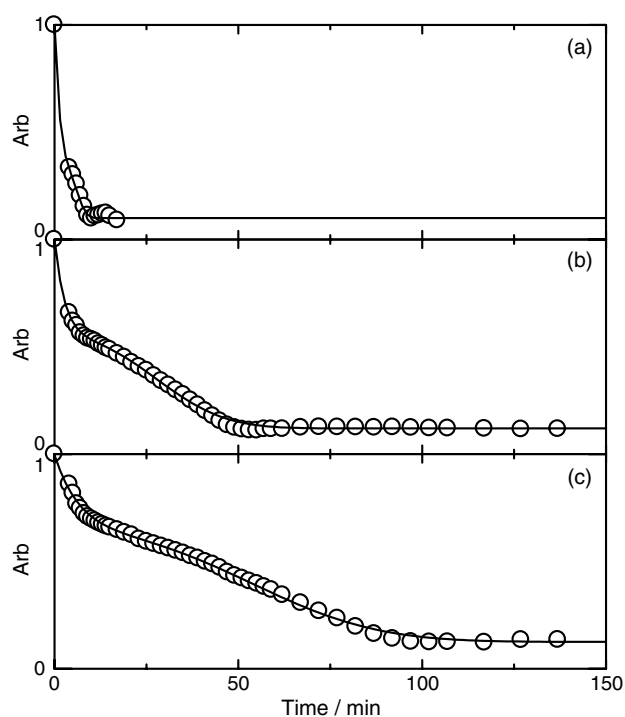


Figure 3. Plots of $S(t)$ as a function of time at $\Delta T = 0.4^\circ\text{C}$. The solid line through the data is a fit to equation (7). The thickness of the gels is (a) 0.1, (b) 0.3 and (c) 0.4 mm.

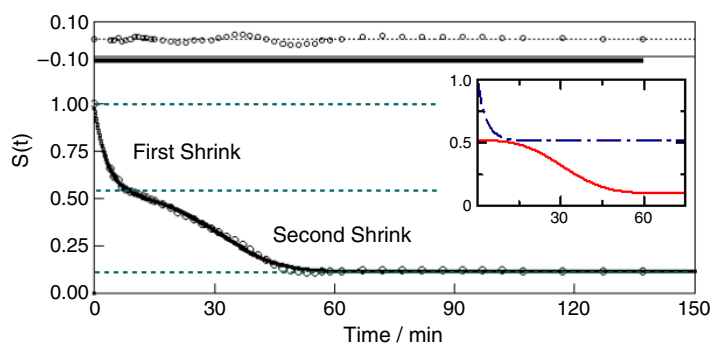


Figure 4. $S(t)$ is plotted as a function of time at $\Delta T = 0.4^\circ\text{C}$. A two-step shrinking is clearly observed. The solid line through the data is a fit to equation (7) and the residuals are shown above as a function of time. The first and second shrinking correspond to the first and second terms of equation (7), respectively, as shown in the inner plot.

and approaches a certain constant value. The timescale of $S(t)$ is elongated with increasing the thickness of gels.

3.2. Curve fitting for the shrinking process of PNIPA gels

A sum of exponential and stretched exponential functions was adequate to fit the time-dependent shrinking process $S(t)$ as shown in figures 3 and 4.

$$S(t) = A_1 \exp\left(-\frac{t}{\tau_1}\right) + A_2 \exp\left(-\left(\frac{t}{\tau_2}\right)^\beta\right) + (1 - A_1 - A_2). \quad (7)$$

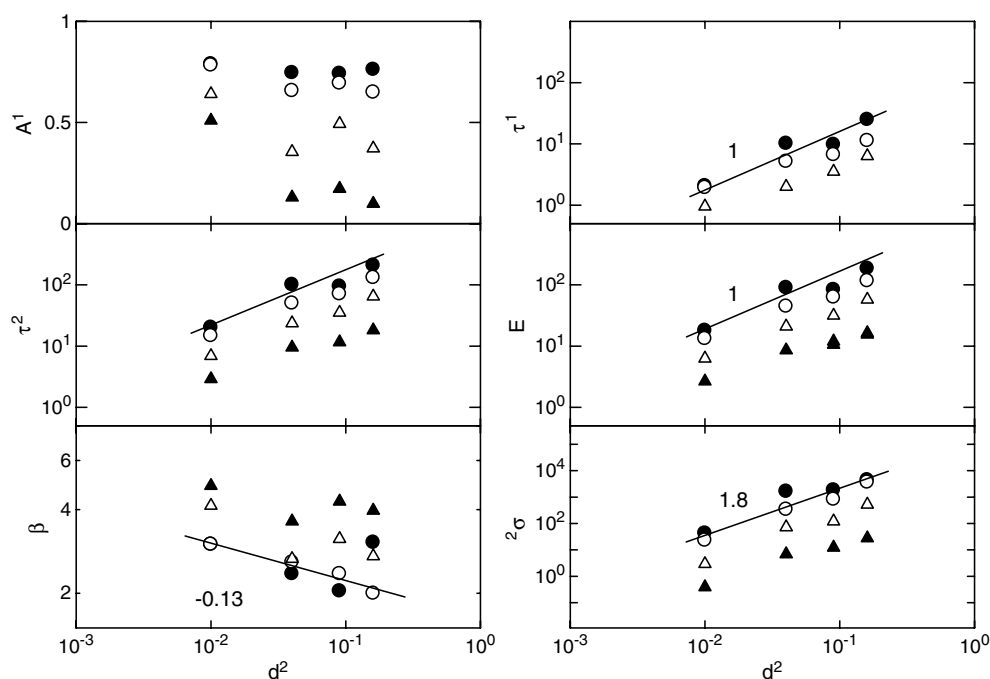


Figure 5. Plots of the square of thickness of gels d^2 versus fitting parameters of equation (7) and their corresponding parameters of $D(\tau)$ (equation (12)) at $\Delta T = 0.0^\circ\text{C}$ (\bullet), 0.2°C (\circ), 0.4°C (Δ) and 1.0°C (\blacktriangle).

Table 1. Fitting parameters of $S(t)$ (equation (7)) and the corresponding characteristic parameters of $D(\tau)$ (equation (12)) at $\Delta T = 0.4^\circ\text{C}$ for gels with various thicknesses d .

d	A_1	τ_1	A_2	τ_2	β	τ_{\max}	E	σ^2
(mm)		(min)		(min)		(min)	(min)	(min ²)
0.1	0.641	0.957	0.247	6.93	4.13	6.48	6.29	2.95
0.3	0.494	3.54	0.389	35.3	3.14	31.2	31.6	121
0.4	0.372	6.36	0.505	64.9	2.72	54.8	57.8	525

The first and second terms correspond to the first and second shrinking processes, respectively. A_1 and A_2 are fractions of each shrinking, and τ_1 and τ_2 are characteristic times of each shrinking. Fitting parameters of equation (7) for various thickness gels are listed in table 1 and plotted against the thickness of gels in figure 5. The numerical value of β is always larger than one. Tanaka *et al* showed that the first shrinking undergoes a diffusion-like process of the polymer network and that the temporal change of gel size is expressed by a single exponential relaxation [17]. They also interpreted the cause of such two-step shrinking as the formation of a ‘skin layer’ which prevents solvents from permeating across the boundary [18]. The ‘skin layer’ has been proposed as a shrunken layer formed on the surface of gels when they shrink and observed by NMR spectroscopy measurement [19] and discussed on the basis of the morphological changes of gels [20]. The two-step shrinking process of PNIPA gels is expressed as follows [15]. PNIPA gels first shrink monotonically, and stop shrinking with skin layer formation on the surface of gels, then the skin layer may break or change, and the inner

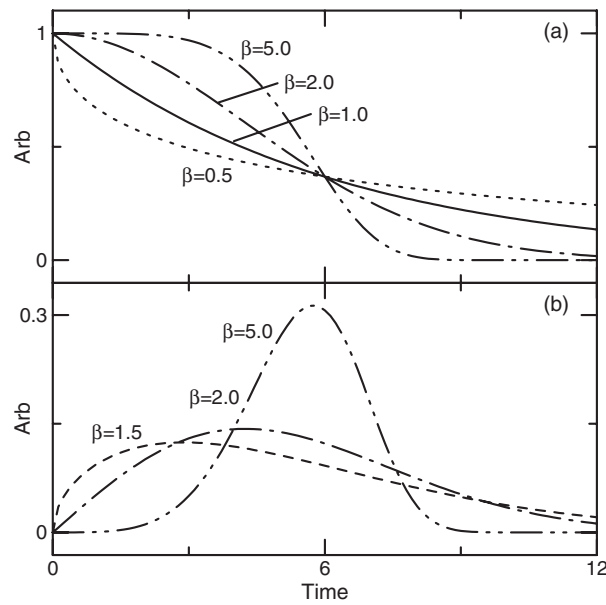


Figure 6. Curves of a stretched exponential function (equation (8)) and its distribution function $D(\tau)$ (equation (12)) at various β with $\tau_2 = 6.0$.

part starts to shrink. $\tau_{\square Q}$ is the characteristic time to collapse the skin layer and β is a degree of the collapse strength of the skin layer.

3.3. Definition of distribution function in stretched exponential function with $\beta > 1$

The following stretched exponential function with $\beta > 1$ was proposed as a part of the fitting function of $S(t)$ in equation (7), that is, the secondary shrinking process of PNIPA gels.

$$I(t) = \exp\left(-\left(\frac{t}{\tau_2}\right)^\beta\right). \tag{8}$$

As shown in figure 6, $I(t)$ decreases monotonically in the case of $0 < \beta < 1$, whereas $I(t)$ remains one for a while and abruptly decreases from one to zero when β is greater than one. Here we incorporate a concept of a superposition of functions using $D(\tau)$ in equation (2) to interpret the stretched exponential function with $\beta > 1$. If the stretched exponential function with $\beta > 1$ (equation (8)) is observed phenomenologically, the derivative of $I(t)$ is given by

$$\begin{aligned} \frac{dI(t)}{dt} &= \frac{d}{dt} \int_0^\infty D(\tau) F(t, \tau) d\tau = \int_0^\infty \left[\frac{d}{dt} (D(\tau) F(t, \tau)) \right] d\tau \\ &= \int_0^\infty \left[\frac{dD(\tau)}{dt} F(t, \tau) + D(\tau) \frac{dF(t, \tau)}{dt} \right] d\tau. \end{aligned} \tag{9}$$

Assuming that $F(t, \tau)$ is expressed by a step (Heaviside) function as

$$F(t, \tau) = 1(t \leq \tau), \quad 0(t \geq \tau), \tag{10}$$

$-dF(t, \tau)/dt$ becomes a δ function and equation (9) can be rewritten as

$$\frac{dI(t)}{dt} = -D(\tau). \tag{11}$$

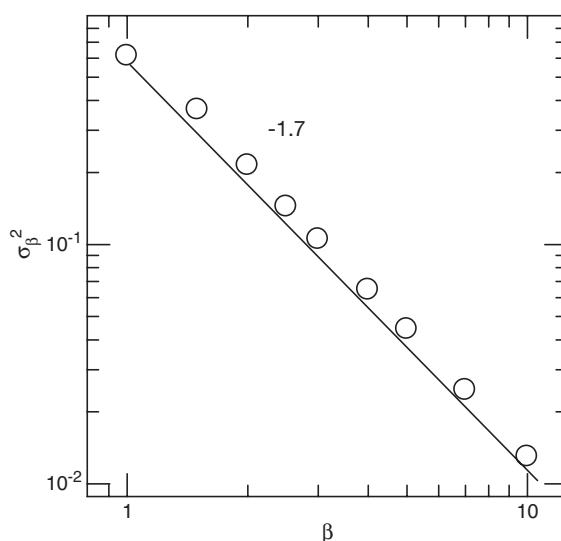


Figure 7. Log–log plot of β versus σ_β^2 .

This indicates that $D(\tau)$ is equal to the derivative of the observed relaxation curve. In the case where $I(t)$ is represented by equation (8), $D(\tau)$ is given by

$$D(\tau) = \frac{\beta}{\tau_2} \left(\frac{\tau}{\tau_2} \right)^{\beta-1} \exp \left(- \left(\frac{\tau}{\tau_2} \right)^\beta \right) (\tau > 0). \quad (12)$$

The properties of this distribution function are shown in the appendix. The average E and the dispersion σ^2 of equation (12) are analytically deduced by (A.7) and (A.9), respectively. To represent the β effect on σ^2 , σ_β^2 is introduced by $\sigma_\beta^2 = \sigma^2/\tau_2^2 = \Gamma[1 + 2/\beta] - \Gamma[1 + 1/\beta]^2$ and plotted as a function of β in figure 7. The fact that $\sigma_\beta^2 \sim \beta^{-1.7}$ holds in the range of β from one to ten indicates that σ^2 can be used instead of β .

This analytical approach holds for any β value in principle. In fact, the β value in this report varies from 2 to 4.5 and is larger than the values which have been reported as follows. To explain the isothermal crystallization of alloy or polymer, a stretched exponential with $\beta > 1$ was derived by Avrami, assuming that crystal particles appear as nuclei and grow with the particle impingement [21]. $\beta - 1$ is a space dimension for nuclear growth, so β itself varies from one to four. On the other hand, a stretched exponential with $\beta = 2$ (Gaussian) is assumed as a good approximation of a relaxation function for the exchange narrowing problem of paramagnetic resonance in the theory of Kubo and Tomita [22]. A stretched exponential function with β ranging between two and three was used in the aggregation and sedimentation behaviours of latex particles [23].

3.4. Shrinking phenomenon of PNIPA gels from the viewpoint of the distribution function

To apply the above analytical method to the secondary shrinking process of PNIPA gels, there are two kinds of interpretations. First, let us imagine that PNIPA gels consist of a lot of parts. Each part of the gels individually undergoes a step-like shrinking at $t = \tau$, and the distribution $D(\tau)$ is expressed by equation (12). Second, it is considered that the secondary shrinking process consists of small steps. Assuming each step-like shrinking is undergone at $t = \tau$, the distribution $D(\tau)$ is expressed by equation (12).

Plots of fitting parameters of equation (7) against the thickness of gels d are shown in figure 5. The characteristic times of shrinking τ_1 , τ_2 and E are proportional to the square of thickness of gels d as τ_1 , τ_2 , $E \sim d^{-2}$. Since the relationship $\tau_1 \sim d^{-2}$ was deduced by combining the shear effect on the diffusion process of first shrinking [17], the fact that not only τ_1 but also τ_2 and E hold such a relationship suggests that the PNIPA gels also shrink as collective diffusion in the secondary shrinking. Certainly, Tomari *et al* showed the secondary shrinking process could be explained by the collective diffusion on assuming the 'skin layer' [24]. Therefore, the secondary shrinking mechanism can be described not by the former step-like shrinking of each small part, but by the latter multi-step shrinking of gels. Note that the latter image of the multi-step shrinking of gels was explained for the first shrinking process by Li *et al* to solve the diffusion equation [17]. Assuming that the skin layer collapses or changes in the secondary shrinking, τ_2 and E are the characteristic and average time to collapse the skin layer. As shown in figure 5, the E value is not very different from τ_2 . The asynchronous value of the distribution β and the dispersion of the secondary shrinking process σ^2 are related to d^2 as $\beta \sim (d^2)^{-0.13}$ and $\sigma^2 \sim (d^2)^{1.8}$, respectively. These relationships can be converted into each other using $\sigma_\beta^2 \beta^{-1.7}$.

4. Conclusion

We have proposed a new mathematical approach to explain the origin of the observed stretched exponential function with β higher than unity. When a stretched exponential function with $\beta > 1$ is phenomenologically observed to express the relaxation process, assuming that the elemental function is expressed by the step (Heaviside) function, the distribution function of characteristic times $D(\tau)$ is analytically deduced as equation (12). The average E and the dispersion σ^2 of $D(\tau)$ are given in equations (A.7) and (A.9), respectively. This concept is applied to the secondary shrinking of PNIPA gels and it can be considered that the gels show multi-step shrinking.

Appendix

If a stretched exponential function with $\beta > 1$ is observed phenomenologically, if the elemental function is step-like, the distribution function of the characteristic time of the step-like process $D(\tau)$ is expressed by equation (12). Here properties of equation (12) will be shown. First the integral value of equation (12) is equal to one as follows.

$$\int_0^\infty D(\tau) d\tau = \left[-\exp\left(-\left(\frac{\tau}{\tau_2}\right)^\beta\right) \right]_0^\infty = 1. \quad (\text{A.1})$$

Let us deduce both the average E and the dispersion σ^2 of $D(\tau)$. In general, E and σ^2 of $D(\tau)$ are evaluated by the following equations.

$$E(\tau) = \int_0^\infty \tau D(\tau) d\tau \quad (\text{A.2})$$

$$\sigma^2(\tau) = \int_0^\infty (\tau - E(\tau))^2 D(\tau) d\tau = E(\tau^2) - E(\tau)^2. \quad (\text{A.3})$$

When $D(\tau)$ is expressed by equation (12), $E(\tau)$ and $E(\tau^2)$ are given by

$$E(\tau) = \int_0^\infty \tau D(\tau) d\tau = \beta \int_0^\infty \left(\frac{\tau}{\tau_2}\right)^\beta \exp\left(-\left(\frac{\tau}{\tau_2}\right)^\beta\right) d\tau \quad (\text{A.4})$$

and

$$E(\tau^2) = \int_0^\infty \tau^2 D(\tau) d\tau = \beta \tau_2 \int_0^\infty \left(\frac{\tau}{\tau_2}\right)^{\beta+1} \exp\left(-\left(\frac{\tau}{\tau_2}\right)^\beta\right) d\tau. \quad (\text{A.5})$$

Substituting $z = \tau/\tau_2$ and using the formula

$$\int_0^\infty z^{b-1} \exp(-az^\alpha) dz = \frac{\Gamma[b/\alpha + 1]}{a^{b/\alpha} b}, \quad (\text{A.6})$$

equations (A.4) and (A.5) are given by

$$E(\tau) = \tau_2 \beta \int_0^\infty z^\beta \exp(-z^\beta) dz = \tau_2 \frac{\beta}{\beta+1} \Gamma\left[\frac{\beta+1}{\beta} + 1\right] = \tau_2 \Gamma\left[1 + \frac{1}{\beta}\right] \quad (\text{A.7})$$

and

$$E(\tau^2) = \tau_2^2 \beta \int_0^\infty z^{\beta+1} \exp(-z^\beta) dz = \tau_2^2 \frac{\beta}{\beta+2} \Gamma\left[\frac{\beta+2}{\beta} + 1\right] = \tau_2^2 \Gamma\left[1 + \frac{2}{\beta}\right], \quad (\text{A.8})$$

respectively. Γ is the gamma function. Therefore, E of $D(\tau)$ was given by equation (12) and σ^2 is written as

$$\sigma^2 = E(\tau^2) - E(\tau)^2 = \tau_2^2 \left\{ \Gamma\left[1 + \frac{2}{\beta}\right] - \Gamma\left[1 + \frac{1}{\beta}\right]^2 \right\}. \quad (\text{A.9})$$

In addition, the time which shows the maximum $D(\tau)$, τ_{\max} , was calculated as

$$\tau_{\max} = \tau_2 \exp(\ln(1 - 1/\beta)/\beta). \quad (\text{A.10})$$

References

- [1] Kohlrausch F 1863 *Ann. Phys. Chem.* **7** 352
- [2] Williams G and Watts D C 1970 *Trans. Faraday Soc.* **66** 80
- [3] Anderssen R S, Saiful A H and Loy R 2004 *J. ANZIAM J.* **E 45** C800
- [4] Evesque U 1983 *J. Physique* **44** 1217
- [5] Humbert P 1945 *Bull. Soc. Math. France* **69** 121
- [6] Chu B, Wang Z and Yu J 1991 *Macromolecules* **24** 6832
- [7] Provencher S W 1979 *Macromol. Chem.* **180** 201
- [8] Havriliak S and Nagami S 1967 *Polymer* **8** 161
- [9] Cole K S and Cole R H 1941 *J. Chem. Phys.* **9** 341
- [10] Davidson D W and Cole R H 1951 *J. Chem. Phys.* **19** 1484
- [11] Rajagopal A K, Ngai K L and Wright G B (ed) 1991 *Relaxations in Complex Systems* (Amsterdam: North-Holland)
- [12] Gomez D and Alegria A 2001 *J. Non-Cryst. Solids* **287** 246
- [13] Sillescu H 1999 *J. Non-Cryst. Solids* **243** 81
- [14] Colmenero J, Arbe A, Alegria A, Monkenbusch M and Richter D 1999 *J. Phys.: Condens. Matter* **11** A363
- [15] Dusek K (ed) 1993 *Adv. Polym. Sci.* **109** 1
- [16] Schild H G 1992 *Prog. Polym. Sci.* **17** 163
- [17] Hashimoto C and Ushiki H 2000 *Polym. J.* **32** 807
- [18] Ushiki H, Rouch J, Lachaise J and Gracia A 1998 *Rep. Prog. Polym. Phys. Japan* **41** 497
- [19] Li Y and Tanaka T 1990 *J. Chem. Phys.* **92** 1365
- [20] Matsuo E S and Tanaka T 1998 *J. Chem. Phys.* **89** 1695
- [21] Yasunaga H, Kobayashi M, Matsukawa S, Kurosu H and Ando I 1997 *Annu. Rep. NMR Spectrosc.* **34** 39
- [22] Sekimoto K 1996 *J. Chem. Phys.* **105** 1735
- [23] Avrami M 1939 *J. Chem. Phys.* **7** 1103
- [24] Avrami M 1940 *J. Chem. Phys.* **8** 212
- [25] Avrami M 1941 *J. Chem. Phys.* **9** 177
- [26] Kubo R and Tomita T 1954 *J. Phys. Soc. Japan* **9** 888
- [27] Hattori Y, Hashimoto C, Lashaise J, Graciaa A and Ushiki H 2004 *Colloids Surf. A* **240** 141
- [28] Tomari T and Doi M 1995 *Macromolecules* **28** 8334